ISSN 0884-5913, Kinematics and Physics of Celestial Bodies, 2016, Vol. 32, No. 2, pp. 55–69. © Allerton Press, Inc., 2016.
Original Russian Text © M.N. Pasechnik, 2015, published in Kinematika i Fizika Nebesnykh Tel, 2016, Vol. 32, No. 2, pp. 3–24.

SOLAR PHYSICS

Spectral Study of a Pair of Ellerman Bombs

M. N. Pasechnik

Main Astronomical Observatory, National Academy of Sciences of Ukraine,
ul. Akademika Zabolotnoho 27, Kyiv, 03680 Ukraine
e-mail: rita@mao.kiev.ua

Received May 15, 2015

Abstract—Results of the analysis of spectral observations of two Ellerman bombs in the H_α line are presented. These bombs (EB-1 and EB-2) appeared and evolved in the active region NOAA 11024 in the emerging magnetic flux area. The spectral data of a high temporal and spatial resolution were obtained with the French–Italian solar telescope THEMIS (Tenerife Island, Spain; THEMIS stands for Télescope Héliographique pour l'Etude du Magnétisme et des Instabilités Solaires) on July 4, 2009. The H_α-line profiles obtained for different periods of the Ellerman bombs (EBs) evolution were asymmetrical, demonstrating the emission excess in the long-wavelength wing. The intensity variations in the line wings indicate both the gradual and pulsed release of energy in the course of EBs. Temporal variations in the line-of-sight velocities V_{los} of the chromospheric material at a level of the Hα-core formation showed two periods in the velocity enhancement, containing several individual peaks. The maximum line-of-sight velocity of the material was –9 and 8 km/s toward and from the observer, respectively. Rapid upward and downward plasma streams (where V_{los} reaches –80 and 50 km/s, respectively) were sometimes observed. The Ellerman bombs were accompanied by small chromospheric ejections (surges) lasting for 0.5–1.5 min. A fine structure of EBs was found in the H_α-line spectra obtained during 4 min, when the intensity in the line wings sharply increased. The peculiarities of variations in the intensity of the H_α-line wings and the line-of-sight velocity of the chromospheric material suggest that two investigated EBs appeared and evolved as a physically connected pair. Our results support the model wherein the magnetic reconnection in the lower atmospheric layers is considered as a triggering mechanism for the EB formation.

DOI: 10.3103/S0884591316020057

INTRODUCTION

As is known, Ellerman bombs (EBs) are short-lived small-scale bright structures in the solar atmosphere; they are connected with a quick local release of energy, magnetic fields, and specific plasma motions. EBs are observed in the wings of strong chromospheric lines and the ultraviolet (UV) continuum. Observations show that Ellerman bombs mostly appear in the young developing active regions (ARs) with a complex magnetic structure, in the regions of emerging magnetic fluxes, and in the vicinity of sunspots. As solar flares, EBs are localized near zeroth lines of the longitudinal magnetic field and in the patches of the magnetic fields of opposite polarity. Though this interesting phenomenon has been in the focus of many studies [1–14, 16–27, 29–39, 41–44], its nature is not completely understood and the physical interpretation still remains vague.

F. Ellerman was the first who paid attention to this phenomenon in the visual and photographic observations of the Sun at the Mount Wilson Observatory; he called it solar hydrogen "bombs" [17]. During his observations on September 21, 1915, a very bright and narrow emission band suddenly appeared in the wings of the H_α hydrogen line; this band expanded to 0.4–0.5 nm on both sides of the line, but did not cross it; in several minutes, the band disappeared. This phenomenon was so highly improbable that it hardly seemed real. However, after the second observations, it became clear that such a phenomenon actually occurs as a component of solar activity. Moreover, it turned out that this phenomenon had been already described before by W.M. Mitchell in his report of the Sun observations at the Harverford College Telescope in 1909. The observations showed that the weaker emission bands appear in the wings of the H_β and H_γ lines as well.

Almost 40 years later, a new stage in the study of Ellerman bombs started at the Crimean Astrophysical Observatory [1, 3, 6–8, 29, 38]. Starting in 1954, A.B. Severnyi and his colleagues obtained a large number of EB spectrograms. The appearance of this phenomenon in the H_α-line spectra gave it one more name—"moustaches." It was determined that most EBs are located beneath filament arc systems absorbing the

radiation, which generates a deep absorption core in the H_α line. It was found that EBs are short-lived formations appearing in the active regions as small bright points. Moreover, in the H_α line, only a blue wing of the moustaches is most often well pronounced, while a red one is at the detection limit. It was supposed that a large extension of the emission wings (0.7–1.0 nm) is caused by the Doppler effect and corresponds to the velocities of several hundreds of kilometers per second and that this phenomenon can be described as an ejection of particles due to a symmetric explosion in the solar atmosphere. A small size of the emission centers pointed to the large density of energy there. To explain the wide emission wings of chromospheric lines, Severnyi proposed the model that considers EBs as compact regions with converging or diverging plasma jets [7, 8, 38].

The main properties of EBs were repeatedly described [19, 26, 27, 30, 33, 35, 42, 44]. It was determined that the typical size and the mean lifetime of EBs are 1″ and 15 min, respectively. However, EBs of approximately 0.3″ in size and less than one minute in lifetime are also observed [33], and there are EBs living longer than an hour and demonstrating the light curves containing several impulses. Very often EBs are accompanied by small chromospheric ejections—surges [18, 31, 32, 44]. As is deemed, this indicates a magnetic reconnection in the lower chromosphere. The profiles of chromospheric lines in the EB spectra are characterized by a strong absorption in the line center and an enhanced emission in the wings (with maxima near ±0.1 and ±0.035 nm from the centers of the H_α and Ca II H lines, respectively) disappearing beyond ±0.5 nm [18, 19, 22, 26, 36, 44]. There are researchers who interpret this fact as evidence of the formation of EBs in the lower atmospheric layers, below the region, where the center of the H_α line is formed in the quiet Sun, and, probably, nearby of the temperature minimum region [11, 12]. EBs are mostly observed in the H_α line, while bright points are also seen in the Ca II H line ($\lambda = 854.2$ nm) and the UV continuum at $\lambda = 160$ nm [3, 12, 20, 23, 25, 32, 36]. The studies showed that the chromospheric Ca II H line is a good indicator of Ellerman bombs and may yield new information on this phenomenon. A fine structure of Ellerman bombs was found [20, 32]. It turned out that they are composed of two components: a central one located along the neutral line of the magnetic field and a diffuse halo. It is believed that EBs is funnel-shaped in structure, i.e., their spatial scale is larger in the chromosphere than in the photosphere [27]. In studies [18, 19], it is concluded that EBs may be called submicroflares, since their energy amounts from 10^{19} to 5×10^{20} J. Moreover, it was found that EBs may generate periodic velocity oscillations along a loop and induce the events of a larger reconnection scale [25].

There are several models explaining the main observed properties of Ellerman bombs. At present, in the mostly developed model, EBs are considered as being formed due to magnetic reconnection in the lower chromospheric layer or the upper photospheric layer, when the material density and the magnetic field strength are high [12, 16, 18, 19, 21, 24, 26, 36, 37, 39, 42]. Both the thermal and nonthermal mechanisms (beams of energetic particles) generating Ellerman bombs are considered, and the magnetic field energy is mainly spent accelerating plasma streams. It is supposed that the EB evolution is accompanied by generation of bidirectional streams originating from the reconnection site. In a paper [31], from the spectral observations of gaseous streams in Ellerman bombs, it was shown that the source of bidirectional streams is between the lower photosphere and lower chromosphere; and it was hypothesized that the magnetic reconnections inducing the formation of Ellerman bomb occur exactly in this atmospheric layer.

In the focus of many studies, there were the velocity and direction of the material motion in the EB evolution regions. According to the estimates in papers [3], [31], and [26, 30], at the chromosphere level, the material moves upward with a velocity of 15–18, 1–3, or 6–8 km/s, respectively. In [39], theoretical calculations yielded a strong downwelling stream with $V_{los} \sim 10$ km/s between the upper photosphere and lower chromosphere. On the other hand, the downwelling streams with velocities ranging from 0.1 to 0.5 km/s were found in the photosphere.

Observations showed that 50% of Ellerman bombs appear and disappear in pairs with components spaced on average by approximately 2200 km [44]. As a rule, in such a pair, EBs synchronously evolve, and the axis of each of the pairs makes a small angle with the magnetic field lines. This phenomenon is believed to be connected with emerging bipolar tubes of the magnetic field.

The purpose of our study is to obtain new observational data on Ellerman bombs. We report the results of the analysis of the spectral observations of two Ellerman bombs that appeared and evolved in the active region NOAA 11024. The peculiarities in the intensity variations of the H_α line in the spectra taken at different stages of the EB evolution were analyzed, and the changes in the line-of-sight velocities of the chromospheric material in the region of Ellerman bombs and their vicinity were studied.

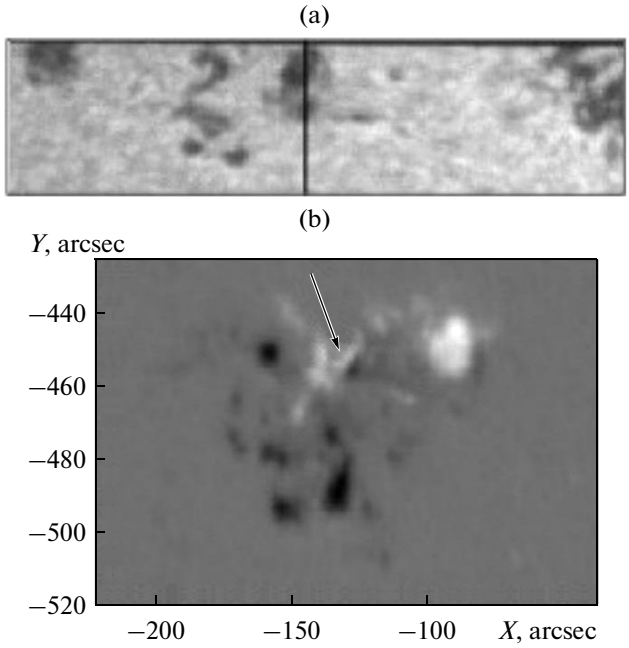

Fig. 1. (a) Area of the analyzed active region NOAA 11024 observed on July 4, 2009; the vertical line is the spectrograph slit position. (b) AR magnetogram obtained with the SOHO/MDI instrument on the day of observations at 9^h36^m UT. The positive and negative polarities are indicated by white and black colors, respectively; arrow points to the analyzed area.

DATA OF OBSERVATIONS

On the day of our observations, July 4, 2009, the active region NOAA 11024 was at an early stage of evolution (it appeared as a plague on June 29), and its activity was quickly growing [4, 28]. The AR area, where the presently analyzed Ellerman bombs had developed, was in the region of one of three currently emerging magnetic fluxes [40]. The group of sunspots was bipolar and contained many inclusions of the elements of opposite polarities located along the axis connecting the main polarities. On the day of observations, the coordinates of the AR were S25E02 (−29″, −449″), i.e., it was near the central meridian of the solar disk, which provided all of the parameters to be determined with no substantial distortion.

In this study, we used the spectral data that were obtained by E.V. Khomenko at the French–Italian 90-cm vacuum telescope THEMIS with high spatial and temporal resolutions. During 20 min (from 9^h30^m to 9^h50^m UT), 400 spectra were acquired with a cadence of approximately 3 s. From them, we used 47 spectra of the best quality.

Figure 1 shows a fragment of the studied AR with a specified position of the spectrograph slit and the magnetogram of the AR obtained with the SOHO/MDI instrument (SOHO and MDI stand for Solar and Heliospheric Observatory and Michelson Doppler Imager, respectively) on July 4, 2009, at 9^h36^m UT. The observed AR area included two pores of opposite polarity. Recall that Ellerman bombs evolve, as flares, in the patches with an opposite magnetic field polarity.

In Fig. 2, the H_α spectra obtained at different moments of observations are presented. In the bottom of one of the first spectra ($9^h30^m56^s$ UT), a band of enhanced brightness is seen. In the same spectrum, the considered AR area is marked by an arrow. In the spectrum obtained at $9^h42^m28^s$ UT, two extended bright narrow emission bands are seen in the wings of the H_α line, while a central part of the line is occupied by absorption; these bands are two Ellerman bombs (EB-1 and EB-2) having developed for that time. The width of the spectrum range containing the H_α line was approximately 0.6 nm. It is seen that the emission in the line wings goes beyond this range; due to this, to determine the widening of the line wings for the time of the EB evolution turned out to be impossible. It is worth noting that the spectra of Ellerman bombs are opposite to the spectra of flares by appearance: in the flares, on the contrary, a strong emission in the center of the H_α line and not very extensive and rather weak wings are observed. In the spectrum obtained at $9^h44^m42^s$ UT, against the background of the emission band in the short-wavelength wing of the H_α line, a small ejection in absorption is seen. It is known that Ellerman bombs are often accompanied by surges.

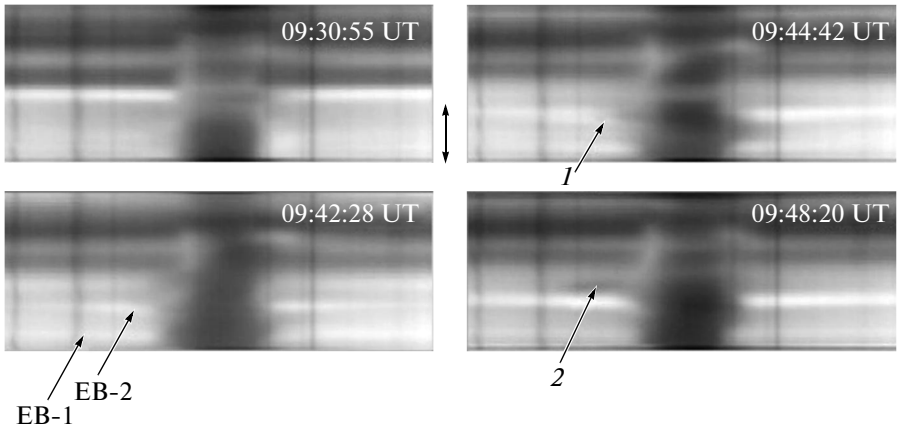

Fig. 2. H_α spectra of the AR obtained at different moments of observations: EB-1 and EB-2 are Ellerman bombs; the analyzed area is marked by an arrow; the chromospheric ejections are labeled by *1* and *2*.

In the spectrum obtained at one of the last moments of observations ($9^h\ 48^m\ 20^s$ UT), one can see only EB-2 and a surge next to it.

VARIATIONS IN THE H_α-LINE INTENSITY AND LINE-OF-SIGHT VELOCITIES

In the study, we used the Stokes I profiles obtained from the spectra with an interval corresponding to the distance of 160 km on the solar surface.

Intensity Variations

In Figs. 3a and 3b, examples of the profiles of the H_α line for two Ellerman bombs are displayed; these profiles correspond to different stages of their evolution. It is seen that the profiles widely diverge in shape and contain several components—wide emission profiles in the wings of the H_α line and an absorption profile in the center of the line. The profiles are asymmetric in intensity and extension of the wings, and the width of the absorption profiles changed in the course of the EB evolution. Figure 3a shows the profiles of the H_α line for EB-1. Profile *1* is given for comparison, it was obtained for the AR area containing no active formations and located beyond the area of an emergent magnetic flux. Profile *2* was obtained from the spectrum for one of the first moments of observations ($9^h30^m56^s$ UT), and the intensity in its wings are higher by approximately 13% as compared to that of profile *1*. At a distance of 0.1 nm from the line core, in the red (long-wavelength) wing, the peak of intensity—the emission component of the profile—is well seen. In profile *3* (the spectrum was obtained 9 min later, at $9^h\ 40^m04^s$ UT), the half-width substantially increased—from 0.11 to 0.15 nm. From the comparison of profiles *2* and *3*, it can be seen that the intensity in the line core decreased, while the intensity in the wings increased. It is also seen that the intensity enhancement in the blue (short-wavelength) wing was gradually spreading along the wing. Moreover, in the red wing, in addition to the intensity enhancement along the wing, the peak of intensity appeared at a distance of 0.11 nm from the center of the line core, as that in profile *2*. Profile *4* (the spectrum was obtained 34 s later) is the widest one; its half-width is 0.17 nm, while the intensity peak in the red wing becomes hardly noticeable at a distance of 0.12 nm from the line center. In the blue wing, the maximum intensity was obtained for profile *5* (the observations were at $9^h42^m45^s$ UT). Its core is asymmetric and shifted toward the blue side, while the intensity in the red wing increased in a farther part of the wing. To the end of observations, the width of the profiles and the intensity in the blue wing started to decrease, while the intensity in the red wing, at a distance of 0.24 nm from the line core, continued growing.

Figure 3b shows the H_α-line profiles for EB-2 and, and for comparison the profile for the quiet Sun from the atlas by Delbouille et al. [15] (profile *1*). It is seen that, in the course of observations, the value of intensity in the line wings in the EB-2 spectra varied more than that in the EB-1 spectra. Profile *2* (the observation moment is $9^h35^m57^s$ UT) corresponds to the early evolution of EB-2, when the brightness in the line wings just started to grow; its half-width is the same as that of profile *1*. In profile *3* (the spectrum was obtained 5^m20^s later, at $9^h41^m17^s$ UT), the intensity increased in the wings and decreased in the core; the profile width increased, and the red wing contains the emission peak at a distance of 0.11 nm from the

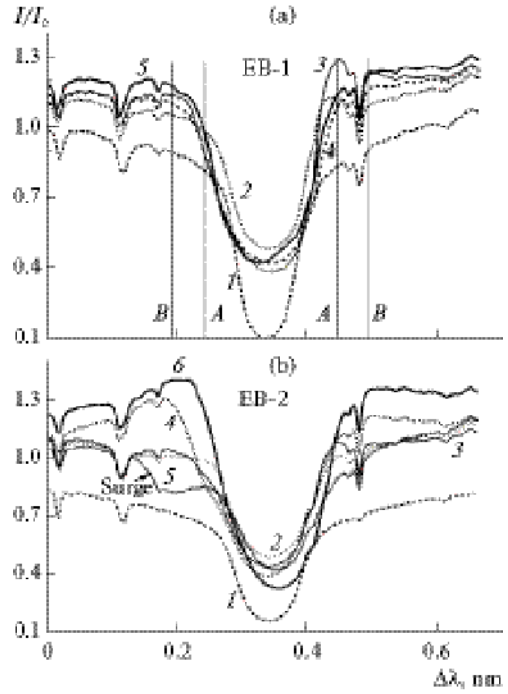

Fig. 3. Profiles of the H_α line for (a) EB-1 (profiles *2–4* are for different moments of observations (see the text) and profile *1* is for the AR area containing no active formations and located beyond the area of an emergent magnetic flux) and (b) EB-2 (profiles *2–5* are for different moments of observations, and profile *1* is for the H_α line of the quiet Sun [15]). Vertical lines *A* and *B* indicate the location of the photometric cross-sections of the spectra at the distances of ±0.1 and ±0.15 nm from the line center.

line core, while the intensity maximum is reached in a farther part of the wing. In profile *4* (the observations were at $9^h44^m02^s$ UT, when the first surge started to develop), the intensity is strongly enhanced in both the blue (the intensity maximum was at a distance of 0.17 nm from the line core) and red wings. The profile widened further; and its half-width, as compared to that of profile *2*, increased from 0.13 to 0.15 nm. It is worth noting that the profiles became wider due to the shift of the blue wing to the short-wavelength side. Profile *5* (the spectrum was obtained at $9^h48^m17^s$ UT) had two absorption components—the main one (EB-2) and the one shifted to the blue side and corresponding to the second ejection. By the shift of this component, the values of V_{los} in the ejection area were determined. Profile *6* (the spectrum was obtained at the last moment of observations, at $9^h49^m34^s$ UT) demonstrates the strongest emission in the wings. In this profile, the core is widest and the whole line is strongly shifted to the red side. It is also seen that this profile is asymmetric: the blue wing is more intense, and the intensity maximum is reached at a distance of 0.15 nm from the center of the line. Note that the red wing was more intense at the beginning of the EB-2 evolution, while the blue one became more intense at the end of observations.

Figure 3 shows how strong the profiles, corresponding to different stages of the evolution of Ellerman bombs, were changing in shape. During this, the changes in the long- and short-wavelength wings were asymmetric. In papers [5, 19, 26], it was supposed that the asymmetry in the wings of the lines' profiles may be caused by the differences in the magnetic field structure and in the density and temperature distributions on the pathways of the streams moving in opposite directions. Thus, one of the plasma streams is directed to the increasing density, while the other one is directed to the decreasing density.

Figures 4a and 4b show the variations in intensity along the spectrograph slit in the wings of the H_α line at a distance of ±0.1 and ±0.15 nm from its center at different moments of observations (cross-sections *A* and *B* in Fig. 3a). Note that, according to the majority of the studies dealing with the EB properties, the intensity in the H_α-line wings reaches its maximum at a distance of ±0.1 nm from the line center. Here, in the blue wing, cross-section *A* is in the internal part of the line wing, while cross-section *B* is in its external part. At the beginning of observations (the moments at $9^h31^m36^s$ and $9^h33^m01^s$ UT), in the spectra related to the area, where Ellerman bombs are formed, the intensity in the H_α-line wings started to increase (curves *1r* and *1b* in Fig. 4a); and the intensity in the red wing was much higher than that in the

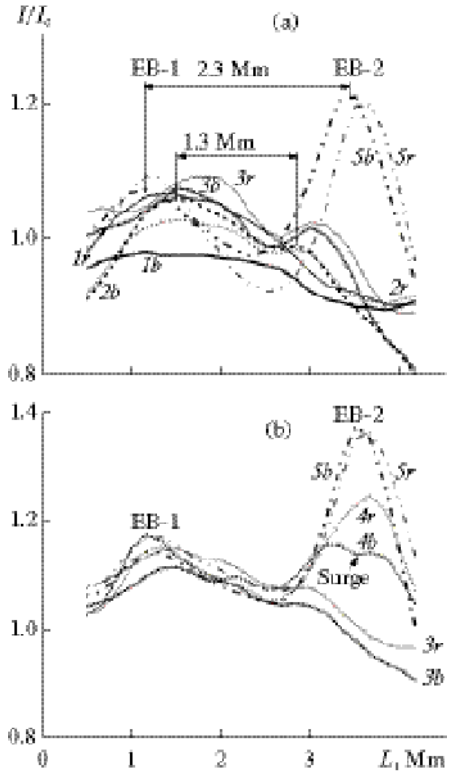

Fig. 4. Intensity variations along the spectrograph slit in the wings of the H_α line at the distances of (a) ±0.1 nm and (b) ±0.15 nm from its center at different moments of observations. Curves *1b*–*5b* and *1r*–*5r* are related to the blue and red wings, respectively, and correspond to five moments of time: $9^h31^m36^s$, $9^h35^m32^s$, $9^h37^m11^s$, $9^h44^m42^s$, and $9^h48^m20^s$ UT.

blue one. In papers [16, 36], it is noted that Ellerman bombs appear in the regions of enhanced brightness. Indeed, after $9^h35^m32^s$ UT, two maxima, corresponding to the evolving Ellerman bombs, started to be clearly pronounced on the curves of intensity (*2r* and *2b*). At that moment of observations, the blue wing was more intense, and the difference in the intensity of the wings was small. It is worth noting that EBs were formed in the regions of intergranular lanes. Granules and intergranular lanes were earlier identified in a paper [28]. In a paper [25], it was hypothesized that Ellerman bombs probably appear due to the strong magnetic fields in the intergranular lanes. As curves *3r*, *3b*, *5r*, and *5b* show, to the end of observations, in the region of the EB-2 formation, the intensity in the H_α-line wings substantially increased and became much higher than that in the region of the EB-1 formation. It is seen that the intensity maxima in the blue and red wings are somewhat shifted relative to each other. Arrows show that the distance L between Ellerman bombs increased for the time of observations from 1.3 Mm at $9^h35^m30^s$ UT to 2.3 Mm at $9^h48^m20^s$ UT.

However, as is seen from Fig. 5, the distance between the Ellerman bombs changed nonuniformly and oscillated with a period of approximately 4 min. The minimum value $L = 1.15$ Mm was at approximately 9^h36^m UT. Then, it started to grow sharply and reached 2.4 Mm in the period of observations from 9^h40^m to 9^h41^m UT; and, from 9^h44^m to $9^h44^m40^s$ UT, its value was largest ($L = 2.52$ Mm) for the period of observations. To the end of observations (from $9^h47^m40^s$ to $9^h49^m30^s$ UT), the value of L decreased to 2.35 Mm. As we will see in the following, ejections of the chromospheric material (surges) occurred, when L increased.

These results are consistent with the data of the other studies. For example, in [44], it was found that the mean distance between the components in a pair is 2.2 Mm. In [25], two magnetic bright points spaced by a distance of approximately 2.7 Mm are described. They moved in opposite directions with a velocity of 2.8 km/s; when the distance between them increased to 4.4 Mm, Ellerman bombs appeared in the H_α line.

Figure 4b shows how the intensity in the wings of the H_α line at a distance of ±0.15 nm from its center changes along the spectrograph slit. It is seen that the intensity in both blue and red wings reached larger values, but the difference between them was smaller than that for ±0.1 nm. In general, the intensity variations mainly demonstrated a very similar behavior for both distances. However, the maxima correspond-

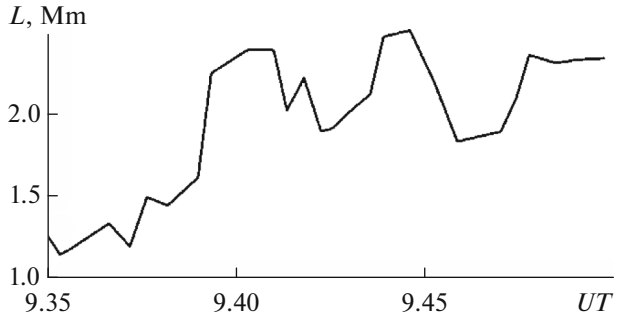

Fig. 5. Temporal variations in the distance between EB-1 and EB-2.

ing to Ellerman bombs became clearly distinguishable later, to the moment of approximately $9^h37^m10^s$ UT (see curves *3r* and *3b*). On curve *4b*, related to the time moment of $9^h44^m42^s$ UT (see also Fig. 2), the decrease of intensity in the EB-2 region corresponds to the chromospheric ejection.

Figures 6a and 6b show temporal variations in the emission intensity of the H_α line in the short-wavelength (*1b* and *2b*) and long-wavelength (*1r* and *2r*) wings at a distance of 0.1 nm (*1b* and *1r*) and 0.15 nm (*2b* and *2r*) from its center and in the center of the line (curves *3*). It is seen that the intensity in the center of the line did not change about (EB-1) or somewhat decreased (EB-2), when the intensity in its wings increased. From this fact it can be inferred that the magnetic reconnections, having resulted in the formation of Ellerman bombs, occurred below the chromospheric layer, where a core of the H_α line is generated. The deeper the reconnection region is in the solar atmosphere, the larger the amount of energy is transferred to the lower atmospheric layers, where the H_α-line wings are generated. In this process, a smaller portion of the energy passes to the higher chromospheric layers, where the H_α-line core is generated. Note that the same relation between the changes of intensity in the wings and the core of the line was obtained in papers [22, 23]. It is seen from Fig. 6 that the intensity variations in the wings were asymmetric and demonstrated the emission excess in the red wing. As a rule, for the majority of Ellerman bombs, the blue wing is more intense; however, as was shown in [18], some EBs demonstrate the same or even higher intensity excess in the red wing than that in the blue one. To explain this phenomenon, it was supposed that such a behavior is connected with dynamical processes taking place in the course of formation and evolution of EBs.

The curves of temporal variations in the EB-1 intensity have three periods of the brightness enhancement that are well seen on all of the curves, and each of the periods contains several individual peaks. For example, the period of the intensity enhancement that lasted for approximately 3 min (from $9^h31^m40^s$ to $9^h34^m20^s$ UT) contained three maxima spaced by an interval of 1 min (at 9^h32^m, 9^h33^m, and 9^h34^m) and well noticeable in both the blue and red wings. It is worth noting that the intensity in the blue wing reached the maximum 10–25 s earlier than that in the red one did. The next period (from $9^h37^m40^s$ to $9^h45^m20^s$ UT) contained five peaks observed with an interval of 1–2 min, and the highest peak in the red wing showed the intensity maximum at $9^h40^m05^s$, while the blue wing contained two high peaks, where the intensity maxima were reached at $9^h42^m45^s$ and $9^h44^m05^s$. The last period started at 9^h47^m UT and contained two peaks spaced by an interval of approximately 2 min. This period was not completely observed, because the observations stopped at 9^h50^m UT. Such peculiarities of the intensity variations in the H_α-line wings indicate that the energy release was impulsive during EB-1.

On the curves of the EB-2 brightness variations, three periods in the intensity enhancement are also distinguishable in the H_α-line wings. During the first period, which lasted for 4 min (from 9^h35^m to 9^h39^m UT), the intensity variations are gentle, while the second and third periods contain several individual peaks, as in the case of EB-1. This testifies to both the pulse and gentle release of energy in the course of EB-2. The second period, which lasted for approximately 5 min (from 9^h41^m to $9^h46^m30^s$ UT), contained three maxima spaced by intervals of 1.5 and 1 min. The third period started at approximately 9^h47^m UT and completely coincided with the corresponding period of EB-1 by the time of reaching the intensity maxima.

The fact that the evolution of the considered Ellerman bombs was accompanied by both the gradual and pulsed release of energy is consistent with the results of [19, 44], as well as with the conclusions of [26, 27, 35, 37] on the origin of Ellerman bombs from successive and discrete magnetic reconnections in the lower chromosphere or upper photosphere.

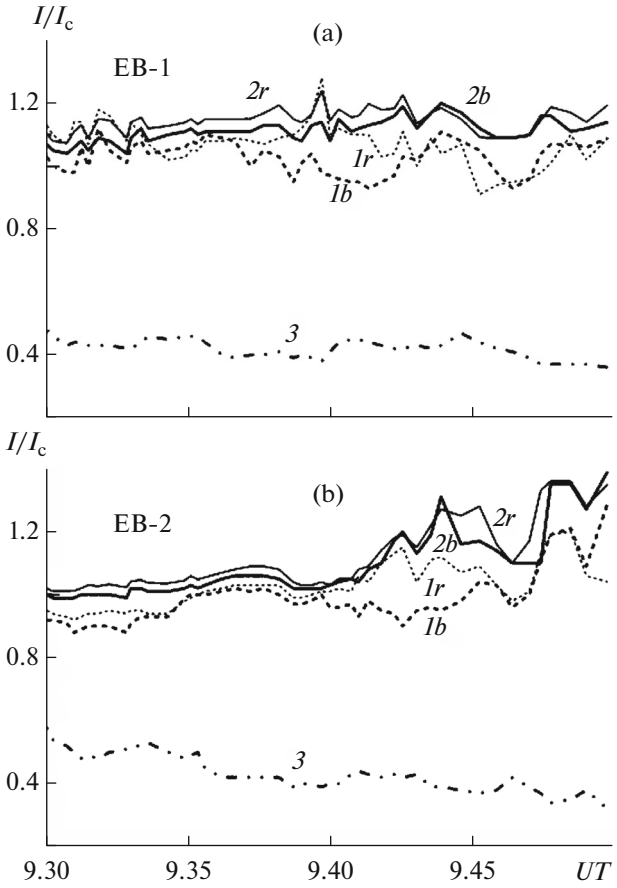

Fig. 6. Temporal variations in the emission intensity in the wings of the H_α line at the distances of ±0.1 and ±0.15 nm from its center in the short-wavelength (curves *1b* and *2b*) and long-wavelength (curves *1r* and *2r*) wings and in the center of the line (curve *3*) for the EB-1 (a) and EB-2 (b) regions.

Line-of-Sight Velocities

As is known, for Ellerman bombs, the profile of the H_α line contains several components: absorption in the line center and emission in the line wings. Each of these components has its Doppler shift that can be used for determining the velocity of the material in the chromospheric layers, where they are generated [10, 13, 26]. Numerical simulations showed that a good fit of the observed profiles by the calculated ones can be reached by varying such physical parameters of the material as the temperature, density, and movement velocity. In the fitting, the change of the velocity field with an altitude in the chromosphere is of key importance, since it controls the shifts and asymmetry of the H_α profiles.

In our study, the line-of-sight velocities V_{los} of the chromospheric material at the level where the H_α-line core is formed were determined from the Doppler shifts of the line core in the spectra relative to its position in the laboratory spectrum with the use of nearby telluric lines. In this procedure, all of the required corrections [4, 28] were taken into account. The error in determining V_{los} was 0.3 km/s.

In Figs. 7a–7c, temporal variations of the chromospheric line-of-sight velocity in the central part of Ellerman bombs and at a distance of 0.33 Mm from it, as well as in the AR between EB-1 and EB-2 are shown; they were determined from the shift of the H_α-line core. For comparison, we show the obtained variations of the line-of-sight velocity in the AR containing no active formations in the period of our observations.

In the AR containing no active formations and beyond the area of an emerging magnetic flux, at a level of generation of the H_α-line core, the chromospheric material moved mostly to the observer; the values of its velocity were between 0.4 and –2.2 km/s, and the velocity varied with a period of approximately 4 min (Fig. 7a, curve *1*).

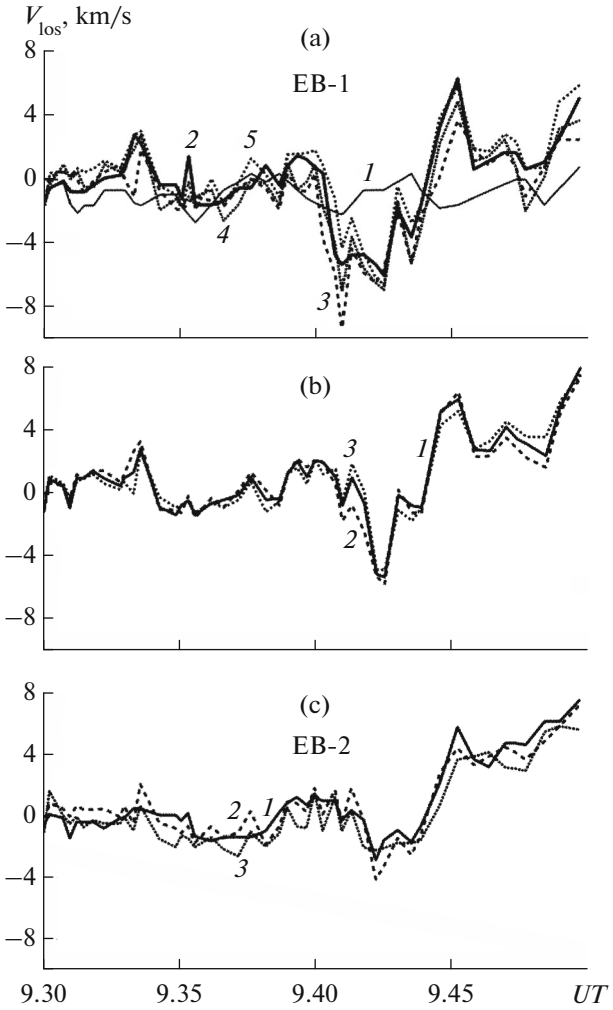

Fig. 7. Temporal variations in the chromospheric line-of-sight velocity of plasma determined from the shift of the H_α-line core: (a) in the central part of EB-1 and at a distance of 0.33 Mm from it (curves *2*–*5*) and in the neighbor AR containing no active formations (curve *1*); (b) in the AR between EB-1 and EB-2; and (c) in the central part of EB-2 and at a distance of 0.33 Mm from it. Negative values of the line-of-sight velocity correspond to the motion toward the observer.

On the curves of the temporal variation of the line-of-sight velocity for EB-1, there are two well-distinguishable time intervals, during which the velocity directed toward and from the observer substantially exceeded the values V_{los} on curve *1* (Fig. 7a). It should be noted that, at the beginning of observations, within a minute at approximately 9^h34^m UT, the material moved downward with a velocity reaching 3 km/s, which was probably connected with magnetic reconnections that occurred from $9^h31^m40^s$ to $9^h34^m20^s$ UT. Later (from $9^h40^m20^s$ to $9^h44^m20^s$ UT), three peaks in the velocity of the material motion toward the observer are seen. For a minute, the velocity sharply increased from 0.5 km/s at $9^h40^m20^s$ UT to –9.3 km/s at $9^h41^m15^s$ UT. The second peak was approximately 1.5 min later, and the maximum velocity reached –7.0 km/s. In another minute, the third peak was observed, and the maximum velocity was –5.2 km/s. After that, the upward motion of the material started to sharply slow down, and, at $9^h44^m20^s$ UT, the upward motion changed into the downward motion; during this time, for a minute, the velocity sharply increased up to 6.5 km/s. Then, the line-of-sight velocity decreased to 0 km/s; and, to the end of observations, it again increased to 6.0 km/s. Note that the velocity of the upwelling chromospheric material was decreasing from the external boundary of EB to the internal one, while the velocity of the material downwelling in this direction was, on the contrary, increasing.

In the AR between the Ellerman bombs (probably, it was a top of the magnetic loop, whose foots were at the places where two considered EBs had developed), the temporal variations of V_{los} were oscillating with a period of approximately 3 min. During the intervals from $9^h31^m50^s$ to $9^h34^m40^s$ UT and from $9^h37^m40^s$ to

$9^h41^m10^s$ UT, the chromospheric material sank with line-of-sight velocities reaching 3.3 and 2.2 km/s, respectively. During the intervals from $9^h34^m40^s$ to $9^h37^m40^s$ UT and from $9^h41^m10^s$ to $9^h44^m00^s$ UT, the material was moving up; in the first interval, V_{los} did not exceed −1 km/s, while the increase of the velocity in the second interval had three maxima: at $9^h41^m20^s$ UT, in 1.5 min, and in another 1 min ($V_{los} = -1.7$, −5.8, and −1.8 km/s, respectively). It is seen that V_{los} reached its maxima approximately 10 s later than that in EB-1, and their values were lower. This means that the excitation spread along the loop from the EB-1 region. At $9^h44^m10^s$ UT, the velocity changed its sign; and the plasma was descending to the end of observations (for approximately 6 min). In this period, three peaks were also noticeable: at $9^h45^m20^s$ UT, in 1.5 min, and in another 2.5 min ($V_{los} = 6.5$, 4.6, and 8 km/s, respectively).

In the EB-2 region, until 9^h36^m UT, there were small oscillations of V_{los} approximately zero; at the moments of $9^h31^m10^s$ and $9^h34^m20^s$ UT, the velocity of the material motion from the observer increased to 2 km/s. Then, two periods 3 min long, from 9^h36^m to 9^h39^m UT and from 9^h39^m to 9^h42^m UT, were observed. During the first period, the chromospheric material moved up with a small velocity, of approximately −2.0 km/s; and, during the second one, V_{los} varied within the limits from −1 to 1.5 km/s. The interval from 9^h42^m to $9^h44^m30^s$ UT, when the material was moving up, had two maxima in the velocity enhancement: to −4.0 and −2.5 km/s. It is seen that the values of the largest velocity became even smaller. At approximately $9^h44^m10^s$ UT, the values of V_{los} changed the sign; at $9^h44^m20^s$ UT, the velocity reached 5.8 km/s. Further, until the end of observations, the material only moved down in this region, and the line-of-sight velocity increased to 7.7 km/s.

The observed temporal changes in the intensity of the H_α line (Fig. 6) and in the line-of-sight velocity of the chromospheric material in the regions of Ellerman bombs (Fig. 7) suggest that EBs appeared and evolved as a physically connected pair. In a paper [44], it is supposed that such Ellerman bombs are formed at the foot points of compact magnetic loops. As a matter of fact, we may observe how the excitations spread from the formation region of EB-1 to that of EB-2, i.e., from one foot of the loop, where EB-1 developed, through the top of the loop to its second foot, the region of the EB-2 evolution. Recall that the analyzed AR was in the area of an emerging magnetic flux [40]. Probably, due to the interaction of the emerging magnetic loop with the already existing magnetic field or the neighbor loop of the serpentine magnetic field, the successive magnetic reconnections occurred in the upper photosphere or lower chromosphere (in the EB-1 evolution region) for the period from $9^h37^m40^s$ to $9^h45^m20^s$ UT (Fig. 6). The plasma streams, upwelling from the reconnection sites, triggered the increase of the line-of-sight velocity of the chromospheric material at a level of the formation of the H_α-line core in the time period from $9^h40^m20^s$ to $9^h44^m20^s$ UT that contained three individual peaks spaced by intervals of 1.5 and 1 min (Fig. 7). It is known that EBs may generate periodic oscillations in the velocity along the loop and induce the repeated reconnections [25]. Thus, as is evidenced by the velocity decrease (Fig. 7), the excitation spread from the EB-1 region and triggered magnetic reconnections in the EB-2 evolution region for the time period from 9^h41^m to $9^h46^m30^s$ that also contained three peaks spaced by the same intervals of 1.5 and 1 min (Fig. 6).

We also determined the line-of-sight velocities of the chromospheric material from the positions of the intensity peaks (emission components) in the H_α-line wings. In Fig. 3, the intensity peaks are well seen in profiles *2* and *3* for EB-1 and profiles *3* and *4* for EB-2. It is worth noting that the intensity peak appeared in the red wing for the EB-1 profiles and in the blue wing for the EB-2 profiles. The emission peaks were distinguishable in the profiles obtained only at some moments rather than in all of the profiles. The emission peak in the red wing of the EB-1 profiles was seen for 2 min at the very beginning of observations, in the period from $9^h31^m$to 9^h33^m UT, and later for 25 s, from $9^h39^m40^s$ to $9^h40^m05^s$ UT. The shift of this peak corresponded to the line-of-sight velocity of 50 km/s. In the blue wing of the EB-2 profiles, the emission peak periodically appeared after $9^h41^m15^s$ UT; its Doppler shift corresponded to V_{los} from −60 to −80 km/s. The obtained results show that downwelling and upwelling high-velocity streams were observed in the regions of Ellerman bombs in some periods of their evolution.

The peculiarities of variations in the line-of-sight velocity of the chromospheric material in the vicinity of Ellerman bombs were also analyzed. In Fig. 8, the change of V_{los} along the AR fragment cut out by the spectrograph slit is presented for different moments of observations. As curve *1* shows, at that time, the material sank with a small velocity of approximately 1 km/s through the whole area of the fragment, while the velocity oscillations not exceeding ±1.5 km/s occurred earlier. Approximately two minutes later (curve *2*), the direction of the chromospheric material movement changed; and the upwelling flux was observed in the whole region ($V_{los} \approx -1$ km/s). It is seen from curve *3* that Ellerman bombs were in the region where the Doppler velocities changed the sign. It is seen from curve *4* that the material were moving up over the whole area,

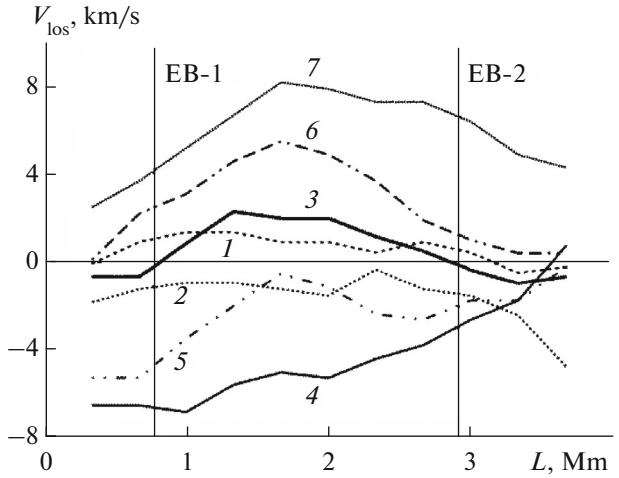

Fig. 8. Variations in the chromospheric line-of-sight velocity along the AR fragment cut out by the spectrograph slit for different moments of observations: $9^h33^m43^s$, $9^h35^m32^s$, $9^h39^m43^s$, $9^h42^m30^s$, $9^h43^m42^s$, $9^h44^m42^s$, and $9^h49^m34^s$ UT (curves *1*–*7*, respectively). Vertical lines indicate the average position of Ellerman bombs.

and the largest velocity (up to −7 km/s) was observed in the EB-1 region, while the values of V_{los} in the EB-2 region were more than two times lower. Curve *5* shows that, to this moment of observations, the velocity of the upwelling movement of the material in the whole area decreased to −5.3 and −2.6 km/s in the EB-1 and EB-2 regions, respectively, and to −0.5 km/s in the region between EBs. A minute later (curve *6*), the direction of V_{los} changed in the whole area: the chromospheric material sank with the largest velocity, to 5.5 km/s, in the region between EBs and with a smaller velocity in the region of Ellerman bombs. To the end of observations, in the investigated area, the sink velocity sharply increased to 4.5 and 7.3 km/s in the EB-1 and EB-2 regions, respectively, and to 8.3 km/s in the region between them.

The analysis of variations in the chromospheric line-of-sight velocity in the investigated area of the AR showed that, in the course of observations, the directions of the material motion changed three times with an interval of approximately 5 min: at $9^h34^m30^s$, $9^h39^m15^s$, and $9^h44^m20^s$ UT. The velocity and direction of the material motion synchronously changed in the whole area. Probably, they were caused by emerging a new magnetic flux. In the vicinity of Ellerman bombs, the material moved slower than in the regions of Ellerman bombs themselves. The strongest variations in the velocity of the material motion, from −5.3 to 8.3 km/s, occurred in the region between the Ellerman bombs. The weakest variations in V_{los} were observed in the EB-2 vicinity. It is worth noting that the value of the line-of-sight velocity of the chromospheric material from the observer was larger between EBs than in the regions of EBs. Probably, this was connected with the magnetic field structure of the investigated area of the AR. Similar results on the velocity variations in the AR area containing the developing Ellerman bombs were obtained in [2, 14]. In a paper [2], from the spectrograms in the H_α line, the chromospheric line-of-sight velocities in the vicinity of six EBs were determined. It was found that the material sank with a velocity ranging from 2 to 10 km/s above five EBs, while the rise was observed only above one EB; the upwelling velocity was 1 km/s, and the sinking velocity reached 17 km/s near EBs. In a paper [14], the upwelling fluxes with a large velocity near bright EBs were obtained; it was also stressed that the velocity field in the vicinity of EBs plays an important role in their generation and evolution.

Velocity of Horizontal Motion of EBs

The distance between Ellerman bombs changed occurred as a result of their horizontal motion. In the considered area of the active region, there were two pores, which allowed us to determine the velocity of horizontal motion of Ellerman bombs relative to them. Both EBs changed the movement direction with a period of approximately 4 min, sometimes approaching, sometimes moving away from each other. In the course of observations, the velocity of horizontal motion of EBs changed from 1 to 9 km/s. It was found in papers [34] and [25] that EBs moved in a horizontal plane with a velocity of approximately 1.1 and 2.8 km/s, respectively, which agrees with our results.

The importance of horizontal motions of plasma for generation and evolution of Ellerman bombs was stressed in many theoretical studies [19, 36, 42]. The modeling showed that the influence of horizontal streams destroys the magnetic configuration stability, which may trigger magnetic reconnections.

Ejections

The Ellerman bombs analyzed in the present paper were accompanied by several small ejections of chromospheric material (surges) that were short in duration—from 0.5 to 1.5 min. In the EB-1 region, two ejections occurred: between $9^h37^m40^s$ and $9^h39^m05^s$ UT and between $9^h46^m25^s$ and 9^h47^m UT. Figure 5 shows that, during the first ejection, the distance between the Ellerman bombs sharply increased and the rising gave place to the sinking of the material (Fig. 7). In the course of both ejections, the EB-1 brightness sharp increased (Fig. 6). In the EB-2 region, there were four ejections during the observations. In the first ejection (at approximately 9^h43^m UT) the distance between Ellerman bombs increased, and the line-of-sight velocity and brightness of EBs also sharply increased. In the spectrum obtained at $9^h44^m42^s$ UT, against the background of the emission band in the short-wavelength wing of the H_α line, the ejection in absorption is clearly seen (Fig. 2): at that time, one of the peaks in the EB brightness enhancement and the change in the direction of the line-of-sight velocity were observed. The third ejection in the EB-2 region occurred simultaneously with the second ejection in the EB-1 region; at that time, one of the peaks in the brightness enhancement was detected. The fourth ejection occurred near EB-2 (Fig. 2, the spectrum was obtained at $9^h48^m20^s$ UT); the highest velocity was –70 km/s in it. It is known that one of the signs of a magnetic reconnection is the generation of surges [18, 31, 32, 44]. In the present paper, we obtained that, at the same time, the distance between EBs, their brightness, and the velocity of chromospheric material increased. Probably, under the influence of horizontal streams (which is evidenced by the change in the distance between Ellerman bombs), magnetic reconnections successively took place, which induced the increase in the brightness of Ellerman bombs and the line-of-sight velocity of the chromospheric material, as well as the formation of surges.

Fine Structure

The studies of the internal structure of the bright points in the Ca II H line that were identified with Ellerman bombs with the use of H_α-images obtained in the line wings (at ± 0.8 nm from the center) showed that they contain two components: the elongated central bright core located along a neutral line of the magnetic field and the diffuse halo [19, 32]. It was found that the subcomponents are smaller than EBs typical size and their lifetime is shorter than the typical one of EBs. The authors explain such a structure of Ellerman bombs by the fact that the reconnection between the already existing field and the emerging magnetic flux of the opposite polarity is not continuous: there are several elemental magnetic reconnections successively occurring one after another and one next to another in space, which induces the ejection of jet-like subcomponents.

In our spectra of EB-2 acquired during the sharp intensity enhancement in the blue wing of the H_α line, from 9^h41^m to 9^h45^m UT, such fine structure is well seen. As Fig. 6 shows, these spectra were obtained at the time of the impulsive energy release, when the magnetic reconnections occurred. In Fig. 9, the distribution of intensity along the spectrograph slit in the blue wing of the H_α line at a distance of 0.1 nm from its center is presented. Curve *1* corresponds to the spectrum obtained at $9^h39^m43^s$ UT and shows the smoothly change of intensity. The intensity peaks corresponding to EB-2 on the other curves contain the main component and one (curves *4* and *5*) or two (curves *2* and *3*) subcomponents. The results we obtained from the EB-2 spectra in the H_α line well agree with the conclusions of papers [19, 32] made from the study of Ellerman bombs in the Ca II H line.

CONCLUSIONS

The analyzed Ellerman bombs evolved in the young active region NOAA 11024 that was at a stage of the rapid growth of activity on the day of our observations, July 4, 2009. Two EBs were formed in the region of one of three currently emerging magnetic fluxes, in the place of the enhanced brightness, and in the intergranular lanes. The H_α-line profiles were asymmetric in length and intensity of the wings, mainly demonstrating the emission excess in the long-wavelength wing. In the course of observations, the distance between the Ellerman bombs increased from 1.3 to 2.3 Mm; it was changing with a period of approximately 4 min rather than uniformly. The velocity of the horizontal motion of Ellerman bombs varied from 1 to 9 km/s.

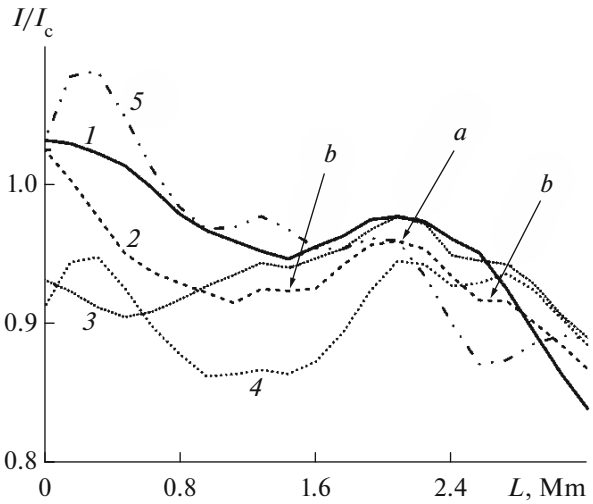

Fig. 9. Fine structure of EB-2. The changes of intensity along the spectrograph slit in the blue wing of the H_α line at a distance of 0.1 nm from its center at different moments of observations (curves *1*–*5*); letters *a* and *b* mark the main component and subcomponents, respectively.

The change of intensity in the H_α-line wings at distances of ±0.1 and ±0.15 nm from the center suggests that both the gradual and pulse release of energy took place in the course of the EBs evolution. When the intensity in the wings of the line increased, the intensity in its center either did not change about (EB-1) or weakly decreased (EB-2).

In the AR area containing no active structures, the velocity of chromospheric material at a level of the formation of the H_α-line core varied in time with a period of approximately 4 min between the limits from 0.4 to −2.2 km/s. In the course of the EBs evolution, the velocity directed toward and from the observer increased to −9 and 8 km/s, respectively. The periods of the velocity growth contained three individual peaks. Sometimes, the plasma streams quickly moving up (to −80 km/s) and down (to 50 km/s) were observed.

During the observations, in the area of the evolution of Ellerman bombs, small ejections of chromospheric material were generated; their lifetime ranged from 0.5 to 1.5 min.

A fine structure of Ellerman bombs was found in the H_α-line spectra obtained for 4 min at the time of the sharp enhancement of intensity in the line wings.

The behavior of variations in the intensity of the H_α-line wings and in the velocity of chromospheric material suggests that two presently analyzed Ellerman bombs appeared and evolved as a physically connected pair.

The data obtained here support the model, where the successive magnetic reconnections in the upper photosphere or lower chromosphere are considered as a mechanism inducing the formation and evolution of Ellerman bombs.

ACKNOWLEDGEMENTS

We are grateful to E.V. Khomenko and R.I. Kostyk for providing us with the data of the THEMIS observations and the codes for their processing.

REFERENCES

1. A. N. Babin, “The size and brightness of whiskers,” Bull. Crimean Astrophys. Observatory **58**, 5–8 (1978).
2. O. E. Den, G. I. Kornienko, F. M. Makhmutov, and F. A. Mikhalina, “The structure of the chromosphere and radial velocities in the vicinity of "moustaches”," Sol. Dannye, No. 11, 85–90 (1983).
3. A. N. Koval’, “On the motions related to moustaches,” Izv. Krym. Astrofiz. Obs. **32**, 32–37 (1964).
4. M. N. Pasechnik, “Plasma motions in the solar loop of emerging magnetic flux,” Kinematics Phys. Celestial Bodies **30**, 161-172 (2014).

5. S. B. Pikel'ner, "The nature of point-sources of lined, continuous and X-ray emission on the Sun," Astron. Zh. **51**, 233–242 (1974).
6. A. B. Severnyi, "Some results of investigations of nonstationary processes on the Sun," Astron. Zh. **34**, 684–693 (1957).
7. A. B. Severnyi, "Investigating the fine structure of the emission of active formations and nonstationary processes on the Sun," Izv. Krym. Astrofiz. Obs. **17**, 129–161 (1957).
8. A. B. Severnyi, *Some Problems of the Solar Physics* (Nauka, Moscow, 1987) [in Russian].
9. V. Archontis and A. W. Hood, "Formation of Ellerman bombs due to 3D flux emergence," Astron. Astrophys. **508**, 1469–1483 (2009).
10. N. Bello González, S. Danilovic, and F. Kneer, "On the structure and dynamics of Ellerman bombs. Detailed study of three events and modelling of H_α," Astron. Astrophys. **557**, A102 (2013).
11. A. Berlicki and P. Heinzel, "Observations and NLTE modeling of Ellerman bombs," Astron. Astrophys. **567**, A110 (2014).
12. A. Berlicki, P. Heinzel, and E. H. Avrett, "Photometric analysis of Ellerman bombs," Mem. Soc. Astron. Ital. **81**, 646–652 (2010).
13. A. Bruzek, "Some observational results on moustaches," Sol. Phys. **26**, 94–107 (1972).
14. H. C. Dara, C. E. Alissandrakis, T. G. Zachariadis, et al., "Magnetic and velocity field in association with Ellerman bombs," Astron. Astrophys. **322**, 653–658 (1997).
15. L. Delbouille, G. Roland, and L. Neven, *Photometric Atlas of the Solar Spectrum from λ3000 to λ10000* (Univ. de LieÌge, Inst. d'Astrophys., LieÌge, 1973).
16. M. D. Ding, J.-C. Henoux, and C. Fang, "Line profiles in moustaches produced by an impacting energetic particle beam," Astron. Astrophys. **332**, 761–766 (1998).
17. F. Ellerman, "Solar hydrogen "bombs "," Astrophys. J. **46**, 298–300 (1917).
18. C. Fang, Y. H. Tang, Z. Xu, et al., "Spectral analysis of Ellerman bombs," Astrophys. J. **643**, 1325–1336 (2006).
19. M. K. Georgoulis, D. M. Rust, P. N. Bernasconi, et al., "Statistics, morphology, and energetics of Ellerman bomb," Astrophys. J. **575**, 506–528 (2002).
20. Yu. Hashimoto, R. Kitai, K. Ichimoto, et al., "Internal fine structure of Ellerman bombs," Publ. Astron. Soc. Jpn. **62**, 879–891 (2010).
21. J.-C. Henoux, C. Fang, and M. D. Ding, "A possible mechanism for the H_α broad wings emission of Ellerman bombs," Astron. Astrophys. **337**, 294–298 (1998).
22. M. Herlender and A. Berlicki, "Spectrophotometric analysis of an Ellerman bomb," Cent. Eur. Astrophys. Bull. **34**, 65–72 (2010).
23. M. Herlender and A. Berlicki, "Multi-wavelength analysis of Ellerman bomb light curves," Cent. Eur. Astrophys. Bull. **35**, 181–186 (2011).
24. H. Isobe, D. Tripathi, and V. Archontis, "Ellerman bombs and jets associated with resistive flux emergence," Astrophys. J., Lett. **657**, L53–L56 (2007).
25. D. B. Jess, M. Mathioudakis, P. K. Browning, et al., "Microflare activity driven by forced magnetic reconnection," Astrophys. J., Lett. **712**, L111–L115 (2010).
26. R. Kitai, "On the mass motions and the atmospheric states of moustaches," Sol. Phys. **87**, 135–154 (1983).
27. R. Kitai and R. Muller, "On the relation between chromospheric and photospheric fine structure in an active region," Sol. Phys. **90**, 303–314 (1984).
28. N. N. Kondrashova, M. N. Pasechnik, S. N. Chornogor, et al., "Atmosphere dynamics of the active region NOAA 11024," Sol. Phys. **284**, 499–513 (2013).
29. A. N. Koval and A. B. Severny, "On the asymmetry of moustaches," Sol. Phys. **11**, 276–284 (1970).
30. H. Kurokawa, I. Kawaguchi, Y. Funakoshi, et al., "Morphological and evolutional features of Ellerman bombs," Sol. Phys. **79**, 77–84 (1982).
31. T. Matsumoto, R. Kitai, K. Shibata, et al., "Height dependence of gas flows in an Ellerman bomb," Publ. Astron. Soc. Jpn. **60**, 95–102 (2008).
32. T. Matsuoto, R. Kitai, K. Shibata, et al., "Cooperative observation of Ellerman bombs between the Solar Optical Telescope aboard Hinode and Hida/Domless Solar Telescope," Publ. Astron. Soc. Jpn. **60**, 577–584 (2008).
33. C. J. Nelson, J. G. Doyle, R. Erdelyi, et al., "Statistical analysis of small Ellerman bomb events," Sol. Phys. **283**, 307–323 (2013).
34. A. Nindos and H. Zirin, "Properties and motions of Ellerman bombs," Sol. Phys. **182**, 381–392 (1998).
35. E. Pariat, G. Aulanier, B. Schmieder, et al., "Resistive emergence of undulatory flux tubes," Astrophys. J. **614**, 1099–1112 (2004).
36. E. Pariat, B. Schmieder, A. Berlicki, et al., "Spectrophotometric analysis of Ellerman bombs in the Ca II, H_α, and UV range," Astron. Astrophys. **473**, 279–289 (2007).
37. J. Qiu, M. D. Ding, H. Wang, et al., "Ultraviolet and H_α emission in Ellerman bombs," Astrophys. J., Lett. **544**, L157–L161 (2000).

38. A. B. Severny, "Mass motions in flares and moustaches indicated by special spectral features," in *Mass Motions in Solar Flares and Related Phenomena: Proc. 9th Nobel Symp., Anacapri, Italy, June 10–12, 1968*, Ed. by Y. Oehman (Almqvist & Wiksell, Stockholm, 1986; Wiley, New York, 1968), p. 71.
39. H. Socas-Navarro, V. Martínez Pillet, D. Elmore, et al., "Spectro-polarimetric observations and non-LTE modeling of Ellerman bombs," Sol. Phys. **235**, 75–86 (2006).
40. G. Valori, L. M. Green, P. Demoulin, et al., "Nonlinear force-free extrapolation of emerging flux with a global twist and serpentine fine structures," Sol. Phys. **278**, 73–97 (2012).
41. G. J. M. Vissers, L. H. M. Rouppe van der Voort, and R. J. Rutten, "Ellerman bombs at high resolution. II. Triggering, visibility and effect on upper atmosphere," Astrophys. J. **774**, 32–46 (2013).
42. H. Watanabe, R. Kitai, K. Okamoto, et al., "Spectropolarimetric observation of an emerging flux region: triggering mechanisms of Ellerman bombs," Astrophys. J. **684**, 736–746 (2008).
43. H. Watanabe, G. Vissers, R. Kitai, et al., "Ellerman bombs at high resolution. I. Morphological evidence for photospheric reconnection," Astrophys. J. **736**, 71–83 (2011).
44. Th. G. Zachariadis, C. E. Alissandrakis, and G. Banos, "Observations of Ellerman bombs in H_α," Sol. Phys. **108**, 227–236 (1987).

Translated by E. Petrova